LSEVIER

Materials Science and Engineering A 442 (2006) 170–174

MATERIALS SCIENCE & ENGINEERING A

www.elsevier.com/locate/msea

Contrasting viscoelastic behavior of melt-free and melt-bearing olivine: Implications for the nature of grain-boundary sliding

Ian Jackson [a,*], Ulrich H. Faul [a], John D. Fitz Gerald [a], S.J.S. Morris [b]

[a] *Research School of Earth Sciences, Australian National University, Canberra, ACT, Australia*
[b] *Department of Mechanical Engineering, University of California, Berkeley, CA, USA*

Received 10 August 2005; received in revised form 4 January 2006; accepted 4 January 2006

bstract

Melt-free and basaltic (complex alumino-silicate) melt-bearing specimens of fine-grained polycrystalline olivine $(Mg_{0.9}Fe_{0.1})_2SiO_4$, tested at gh temperature and low frequency in torsional forced oscillation and microcreep, display markedly different behavior. For the melt-bearing aterials, superimposed upon the high-temperature background is a dissipation peak whose height varies systematically with melt fraction that is ributed to elastically accommodated grain-boundary sliding facilitated by the rounding of grain edges at melt-filled triple junctions. The melt-free aterials display only the high-temperature background dissipation associated with transient diffusional creep—elastically accommodated sliding idently being inhibited by their tight grain-edge intersections. These and similar observations for other ceramic materials require that the classic eory of grain-boundary sliding be revisited and suitably modified.
2006 Published by Elsevier B.V.

ywords: Grain boundaries; Grain-boundary sliding; Mechanical spectroscopy; Partial melting

Introduction

The need to interpret pronounced variations in seismic wave eeds and attenuation in the Earth's upper mantle, dominated by e mineral olivine $(Mg,Fe)_2SiO_4$, motivated a recent laboratory udy of the mechanical behavior of this material. We have fabri- ted fine-grained olivine polycrystals by hot-isostatic-pressing both natural and synthetic (sol–gel) olivine precursors with d without added basaltic melt glass. The resulting specimens ve been mechanically tested with torsional forced-oscillation d microcreep methods under conditions of simultaneous high essure (200 MPa) and temperature (to 1300 °C).

The melt-free and melt-bearing specimens display quali- tively different behavior [1,2]. For the melt-free materials ere is no evidence of a strain-energy dissipation peak. The havior is that described as 'high-temperature background']—a viscoelastic absorption band within which dissipation ries monotonically with temperature and oscillation period th concomitant dispersion of the shear modulus. In marked ntrast, the melt-bearing materials invariably display a broad dissipation peak superimposed upon a melt-enhanced background.

These findings, which have close parallels in recent work on other fine-grained ceramic materials, help clarify the nature of the progressive transition at high temperature from elastic through anelastic to viscoelastic behavior and invite re-examination of the classic literature on grain-boundary sliding.

2. Mechanical spectroscopy of melt-free and melt-bearing polycrystalline olivine

2.1. Experimental and analytical procedures

Specimens recovered after hot-isostatic pressing at 200 MPa and 1200–1300 °C were precision ground to cylindrical shape, enclosed within metal foil (Fe or $Ni_{70}Fe_{30}$), and mounted between torsion rods of high-grade polycrystalline alumina for the torsional forced-oscillation and microcreep tests. The entire assembly is enclosed within a mild-steel sleeve sealed with O-rings at either end in order to exclude the argon pressure medium; this arrangement ensures that the optically flat interfaces within the assembly, across which the torque is transmitted, experience a normal stress equal to the confining pressure. The experimental

Corresponding author. Tel.: +61 2 61252498; fax: +61 2 61258253.
E-mail address: ian.jackson@anu.edu.au (I. Jackson).

21-5093/$ – see front matter © 2006 Published by Elsevier B.V.
:10.1016/j.msea.2006.01.136

apparatus and procedures have been described in detail elsewhere [4,5].

Both hot-pressed and mechanically tested specimens have been characterized by light and electron microscopy and infrared spectroscopy. In particular, grain-size distributions have been determined from lattice orientation maps derived by electron-backscattered diffraction in scanning electron microscope and grain-boundary regions have been imaged and subjected to energy-dispersive chemical analysis in a 300 kV transmission electron microscope.

Mechanical testing of each specimen started with annealing at the highest temperature (usually either 1200 or 1300 °C) and 200 MPa pressure—in order to heal any thermal microcracks and optimize mechanical coupling between torsion rods and specimen. A progressive reduction in compliance and dissipation towards stable values was usually observed over several tens of hours. Once such asymptotic behavior had been established, the assembly was slowly cooled through 50 or 100 °C intervals to room temperature. At each stage, isothermal forced-oscillation tests at selected periods of 1–100 (or 1000 s) and microcreep measurements were performed. Maximum stress amplitudes < 0.3 MPa correspond to maximum shear strains $<5 \times 10^{-5}$—demonstrated to be within the realm of linear viscoelasticity.

2.2. Melt-free olivine specimens

The strain-energy dissipation Q^{-1} (and shear modulus G) data from forced-oscillation tests on melt-free specimens display the monotonic variation with oscillation period and temperature characteristic of the high-temperature background (e.g., Fig. 1a). The Q^{-1} data are well described by an Andrade-pseudoperiod model in which the 'pseudoperiod' master variable

$$X_B = T_o\left(\frac{d}{d_r}\right)^{-m} \exp\left[\left(\frac{-E_B}{R}\right)\left(\frac{1}{T}-\frac{1}{T_r}\right)\right], \quad (1)$$

(with $m = 1$, cf. [6] replaces period T_o in the complex compliance given by Laplace transform of the well-known Andrade creep function

$$J(t) = J_U + \beta t^n + \frac{t}{\eta}. \quad (2)$$

The variables T_r and d_r are suitable reference values of temperature and grain size respectively. This approach accommodates both the anelastic and viscous components of the strain (evident in complementary torsional microcreep records). For essentially anelastic conditions, not too far in period-temperature-grain size space beyond the breakdown of elastic behavior, where the Andrade transient creep term dominates over the viscous term, Q^{-1} varies approximately as βT_o^n. For the Andrade-pseudoperiod model this becomes $Q^{-1} \sim [T_o d^{-m} \exp(-E_B/RT)]^n$. Least-squares fitting of data for a suite of three melt-free specimens of mean grain size 3–23 μm with m fixed at 1 yielded optimal values of $n = 0.28$ and $E_B = 400$ kJ mol^{-1} [1].

2.3. Melt-bearing olivine polycrystals

For the melt-bearing specimens the observed dissipation reflects the superposition of a broad dissipation peak upon a monotonically frequency and temperature-dependent background (Fig. 1b). It is evident that the dissipation peak moves systematically to longer period with decreasing temperature—from <1 s at 1300 °C to ~300 s at 1000 °C.

The broad dissipation peak has been modeled by a Gaussian function of the form

$$Q_P^{-1} = B \exp\left(\frac{-z^2}{2}\right); \quad z = \frac{(\ln X_P - \mu)}{\sigma}; \quad B = B_o \phi^l. \quad (3)$$

The peak pseudoperiod X_P is defined analogously to X_B above and ϕ is the alumino-silicate melt fraction. Dissipation data for temperatures of 1000–1300 °C and oscillation periods of 1–1022 s for a suite of six melt-bearing olivine specimens, of mean grain size 7–52 μm and melt fraction 0.0001–0.037, have been successfully represented as the sum of a Gaussian pseudoperiod peak and the Andrade-pseudoperiod background described above [1].

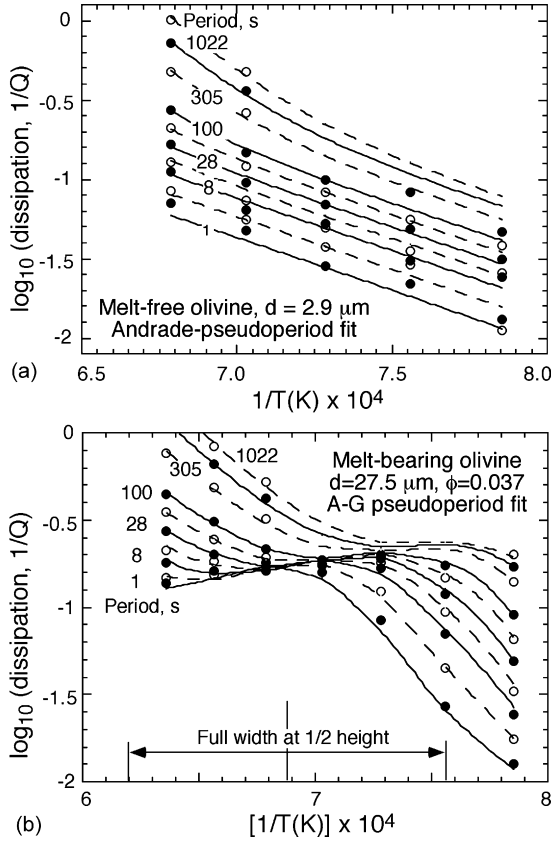

Fig. 1. Contrasting patterns in representative dissipation data (plotting symbols) from torsional forced-oscillation tests on melt-free (a) and melt-bearing (b) olivine polycrystals. The background-only behavior of the melt-free material is fitted to an Andrade-pseudoperiod fit (solid and broken curves for alternate oscillation periods) whereas the background-plus-peak dissipation of the melt-bearing specimen is similarly represented by an Andrade–Gaussian-pseudoperiod model (A–G) as described in the text (redrawn after [1]).

The Q^{-1} data are compatible with an exponent $m = 1$ for the ain-size sensitivity of both X_B and X_P, which provides a match the mild grain-size sensitivity of the background dissipation $Q_B^{-1} \sim (T_o/d)^{0.28}$] and a linear isothermal variation of peak riod with grain size. The strong temperature sensitivity of ak position (period) is expressed in a high activation energy ~720 kJ mol^{-1} [1].

Models for grain-boundary sliding

Grain-boundary sliding has been widely modeled as a plausie mechanism for the ubiquitous transition from elastic through elastic to viscous behavior in fine-grained ceramic materis. Relaxation of boundary-parallel shear stresses within a thin ain-boundary region of low viscosity facilitates sliding accomnied and opposed by growth of a distribution of normal stress rpendicular to the boundary and concentrated at sharp grain ges. The elastic regime prevailing *following completion of astically accommodated sliding* was analyzed in the classic ork of Raj and Ashby [7]. The component of the normal ress parallel to the mean direction y of the grain boundary d integrated over the wavelength λ of the periodic boundy balances the externally applied shear stress τ_a. The elastic rains caused by the newly created distribution of normal stress e those required to restore grain shape compatibility across e slipped boundary. With the boundary topography $x(y)$ for a o-dimensional array of hexagonal grains (of unrelaxed shear odulus G_U and Poisson's ratio ν) represented by a Fourier ries

$$= \sum_{j=1}^{\infty} h_j \cos\left(\frac{2\pi jy}{\lambda}\right), \tag{4}$$

e following expressions for the normal stress σ_n and the equirium distance U of reversible sliding were obtained [7]

$$= -\tau_a\lambda \frac{\sum_{j=1}^{\infty} j^2 h_j \sin(2\pi jy/\lambda)}{\left[\pi \sum_{j=1}^{\infty} j^3 h_j^2\right]},$$

$$= \frac{(1-\nu)\lambda^3 \tau_a}{\left[2\pi^3 G_U \sum_{j=1}^{\infty} j^3 h_j^2\right]}. \tag{5}$$

umerical results, apparently based on truncation of the infinite ries after $N = 100$ terms, yielded a finite sliding distance and a rresponding large anelastic relaxation strength

$$= 0.57(1-\nu) \tag{6}$$

about 0.42 for $\nu = 0.26$ (for olivine at 1000–1300 °C) indendent of grain size. The relaxed shear modulus G_R and the ight Q_D^{-1} of the Debye dissipation peak (as appropriate for e standard anelastic solid) are given by the following expresons

$$\frac{R}{U} = \frac{1}{(1+\Delta)}; \quad Q_D^{-1} = \frac{(\Delta/2)}{(1+\Delta)^{1/2}}. \tag{7}$$

owever, since $h_j \sim j^{-2}$ [8], the infinite sum $\sum j_3 h_j^2$ in the nominators of Eqs. (5) fails to converge—suggesting that

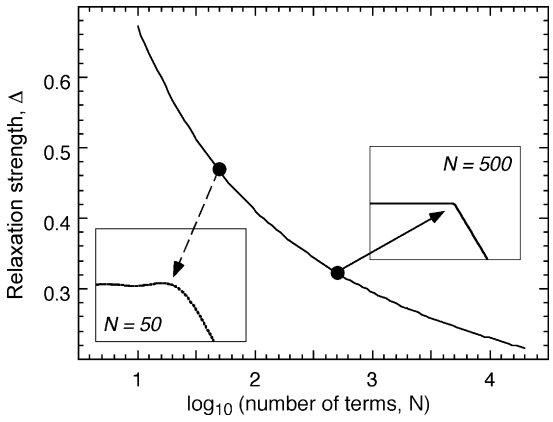

Fig. 2. The effect on the inferred anelastic relaxation strength Δ of truncation after N terms of the Fourier series representing grain-boundary topography and the boundary-perpendicular normal stress in the Raj and Ashby model [7] for elastically accommodated grain-boundary sliding. The insets show the associated rounding of the corners of nominally hexagonal grains.

sufficiently sharp grain edge intersections might inhibit elastically accommodated sliding [2]. The higher values of $\Delta \sim 0.8$ obtained in the modeling of sliding between spherical grains [9,10] and the lower value (0.23) reported from a finite-element study with a fine mesh [11] are consistent with this suggestion. So too is the trend shown in Fig. 2 whereby the relaxation strength inferred from the Raj and Ashby [7] model decreases towards zero with increasing number N of terms in the Fourier series (Eq. (4)) representing the grain-boundary topography.

Mosher and Raj [12] estimated the time-dependent displacement during elastically accommodated sliding by eliminating τ_a between Eqs. (5) above. In this and other studies it has been consistently inferred that the characteristic relaxation time for elastically accommodated grain-boundary sliding is of the form

$$\tau_e = \frac{\eta_b}{G_U \alpha_b}, \tag{8}$$

where $\alpha_b = \delta/d$ is the aspect ratio of the grain-boundary region of thickness δ for grain size d [3,10–13].

The possibilities of elastic and steady-state diffusional accommodation of grain-boundary sliding were examined separately by Raj and Ashby [7]. Grain-boundary sliding with *sequential* occurrence of elastic and diffusional accommodation was explored by Raj [8] in his analysis of transient diffusional creep. The transient required to adjust the normal stress distribution from that prevailing on completion of elastically accommodated sliding (Eq. (5)) to that required for steady-state diffusional creep is of approximate duration

$$\tau_d = \frac{(1-\nu)kTd^3}{[40\pi^3 G_U \delta D_b \Omega]}. \tag{9}$$

Ω is the molecular volume of the diffusing species and D_b is the grain-boundary diffusivity. The transient creep rate calculated by Raj is enhanced relative to the corresponding steady-state diffusional creep rate by a numerical factor that varies approximately as $(t/\tau_d)^{-1/2}$, which integrates to a creep function of the Andrade form (Eq. (2))—as recognized and emphasized by Gribb and Cooper [14]. Accordingly, the diffusional creep tran-

sient should be responsible for a wide absorption band, within which [2,14]

$$Q^{-1} \sim T_o^{1/2} d^{-3/2}. \quad (10)$$

4. Differences between experimental observations and theoretical predictions

Unfortunately, this attractively comprehensive model [7,8,12] of the transition from elastic through anelastic to viscous behavior is difficult to reconcile with the accumulating experimental observations for ceramic and geological materials as follows.

4.1. Melt-free and melt-bearing olivine

For melt-free olivine Q^{-1} varies monotonically across wide ranges of frequency and temperature – without any resolvable dissipation peak that is the signature of elastically accommodated grain-boundary sliding expected from theory. Moreover, the observed dissipation background involves much milder absolute power-law sensitivities (∼1/4) to the variation of period and grain size than the values near 1/2 and 3/2, respectively, prescribed by the theory of transient diffusional creep (Eq. (10)) [8].

For polycrystalline olivine, the presence within grain-edge triple-junction tubules of a volumetrically minor basaltic melt phase or its very fine-grained crystallization products, is correlated with the presence of a dissipation peak superimposed upon a high-temperature background enhanced relative to that of the melt-free equivalent. The peak width exceeds that of the Debye peak of the standard anelastic solid by about 2 decades in period, is independent of temperature but varies mildly with the breadth of the grain-size distribution. The peak height B is well described by power-law dependence upon maximum melt fraction. The peak position (period) varies exponentially with $1/T$ (with a high activation energy E_P of 720 kJ mol^{-1}—possibly reflecting both thermal and compositional influences upon viscosity) and linearly with grain size. This grain size sensitivity is that expected of elastically accommodated sliding (Eq. (8)).

The melt phase in olivine aggregates does not wet grain faces—being confined to an interconnected network of grain-edge triple junctions and larger pockets. The possibility that the dissipation peak reflects the stress-induced redistribution of melt between intergranular ellipsoidal or grain-edge tubular inclusions [13,15] has been considered [2]. However, for the bulk basaltic melt viscosities (1–100 Pa s) appropriate for 1200–1300 °C and the observed aspect ratios of the melt inclusions, estimated relaxation times are generally substantially less than the shortest observed peak-center period (∼0.01 s for 10 μm grain size and 1300 °C). Also, the relaxation strength Δ expected for squirt between grain-edge tubules is too small by an order-of-magnitude to explain the height of the observed dissipation peak and associated dispersion. It was accordingly concluded that melt squirt doesn't offer a plausible explanation of the observed relaxation [2].

Away from the grain-edge triple junctions, the grain-boundary regions of low mean inner potential [16] are of similar width (∼1 nm; Fig. 3) and broadly similar chemical composition in both melt-free and melt-bearing materials. Accordingly we have argued that the effective grain-boundary viscosity is not systematically altered by the presence of the melt phase. Instead,

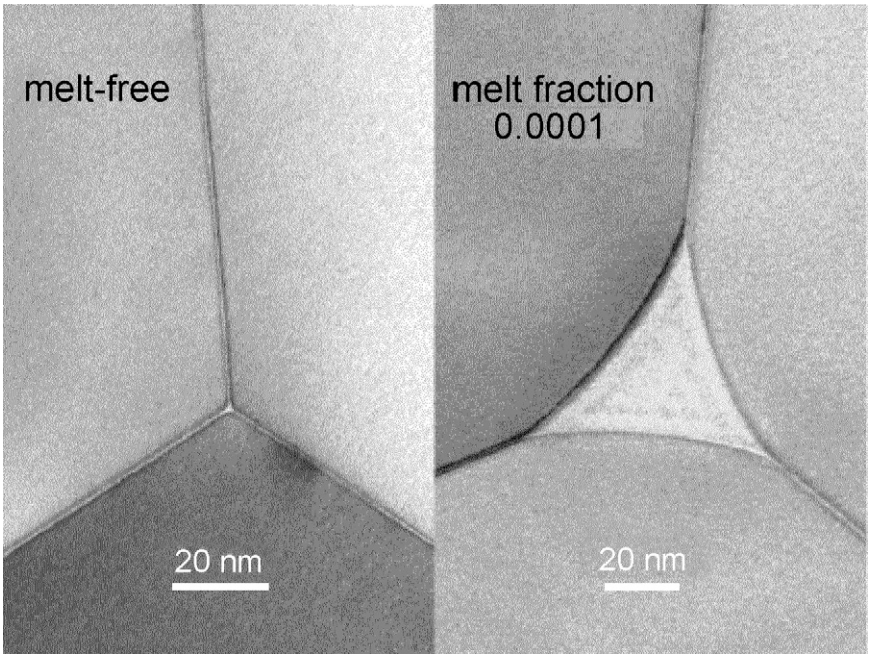

Fig. 3. Typical grain-boundary and grain-edge microstructures in (a) a melt-free olivine specimen and (b) a specimen containing a melt fraction of only 0.0001. Grain-boundary regions of low inner potential and ∼1 nm width, and varying chemical complexity, were imaged and analyzed in both types of material. Although the actual melt fraction is modified by progressive crystallization during staged cooling, the grain-edge triple junctions retain their morphology. In some cases the amorphous melt phase is largely replaced by a nanocrystalline assemblage also plausibly of relatively low viscosity (redrawn after [2]).

e attribute the Q^{-1} peak to the facilitation of elastically accom-odated grain-boundary sliding by the rounding of grain edges the melt-filled triple junctions (Fig. 3). The grain-boundary scosity required to reconcile the location of the observed dis-pation peak with elastically accommodated sliding (Eq. (8)) ries from 10^4 Pa s at 1300 °C to 10^9 Pa s at 1000 °C [2]. hese values are, reasonably, substantially higher than those r bulk basaltic melt (given above) but still much lower than ose (10^{12}–10^{14} Pa s) determined for the melt-bearing olivine ecimens in torsional microcreep tests.

The absence of a dissipation peak for the melt-free olivine lycrystals is tentatively attributed to the role of tight grain-ge intersections, described by short-wavelength terms in the urier series representation of grain-boundary topography, in eventing sliding with elastic accommodation. The stress con-ntrations at grain edges that inhibit elastically accommodated ding are presumably eroded by diffusion on progressively eater spatial scales with increasing period and/or temperature sulting only in the high-temperature background.

2. Other ceramic materials

The presence or absence of a secondary amorphous (usually ica-rich) phase is responsible for similar differences in echanical behavior for a wide range of refractory ceramic aterials. The occurrence of well-resolved dissipation peaks g. in Si_3N_4) has been correlated with the presence of triple-nction tubules of glassy material; the absence of a glassy condary phase from triple-junction tubules and/or grain undaries (e.g. zirconia and alumina) results instead in the ominance of the monotonic background [17,18]. Commercially ailable silicon nitride and silicon carbide typically include secondary siliceous phase occupying an interconnected net-ork of grain-edge tubules and some larger pockets, as well as rming a continuous layer ∼1 nm thick on the grain boundaries 9,20]. Superimposed upon the background for the silica-aring materials is a broad dissipation peak, which like those r our melt-bearing olivine specimens, moves systematically shorter period with increasing temperature without changing height or width. The dissipation peak is normally attributed elastically accommodated grain-boundary sliding (e.g. [20]. owever, several aspects of the observations including the latively low relaxation strength (0.01–0.02) and the close rrespondence of the inferred viscosity with that for bulk amor-ous silica might be more easily reconciled with melt squirt tween grain-edge tubules [2]. In marked contrast, specially epared dilute sialon and silicon carbide materials [21,22] ssessing tight grain-edge intersections and grain boundaries ostly free of the nm-thick silica-rich film, like our melt-free olivine materials, display no dissipation peak—only the mono-tonically frequency- and temperature-dependent background.

5. Conclusions

The contrasting mechanical behavior observed in torsional forced oscillation/microcreep tests on fine-grained olivine poly-crystals with and without small fractions of basaltic melt forms part of a consistent pattern for refractory ceramic materials more generally. In the absence of a secondary grain-boundary phase of low-viscosity, tight grain-edge intersections apparently inhibit the elastically accommodated sliding modeled by Raj and Ashby. Such sliding is evidently facilitated by the rounding of grain edges at triple-junction tubules caused by the presence of a secondary phase of low viscosity. The high-temperature background in both types of fine-grained material is presumably attributable to transient diffusional creep. Such observations require modification of the classic theory of grain-boundary sliding—specifically the analysis of transient diffusional creep without prior elastically accommodated sliding, and exploration of the feasibility of a (concurrent) mix of elastic and diffusional accommodation.

References

[1] I. Jackson, U.H. Faul, J.D. Fitz Gerald, B.H. Tan, J. Geophys. Res. 109 (2004) B06201 doi:10.1029/2003JB002406.
[2] U.H. Faul, J.D. Fitz Gerald, I. Jackson, J. Geophys. Res. 109 (2004) B06202 doi:10.1029/2003JB002407.
[3] A.S. Nowick, B.S. Berry, Anelastic Relaxation in Crystalline Solids, Academic Press, New York, USA, 1972, 677 pp.
[4] I. Jackson, M.S. Paterson, PAGEOPH 141 (1993) 445–466.
[5] I. Jackson, in: S. Karato, A.M. Forte, R.C. Liebermann, G. Masters, L. Stixrude (Eds.), Mineral Physics and Tomography from the Atomic to the Global Scale, AGU, Washington, USA, 2000, pp. 265–289.
[6] T. Kê, Phys. Rev. 72 (1947) 41–46.
[7] R. Raj, M.F. Ashby, Metall. Trans. 2 (1971) 1113–1127.
[8] R. Raj, Metal. Trans. A 6A (1975) 1499–1509.
[9] C. Zener, Phys. Rev. 60 (1941) 906–908.
[10] T. Kê, Phys. Rev. 71 (1947) 533–546.
[11] F. Ghahremani, Int. J. Sol. Struct. 16 (1980) 825–845.
[12] D.R. Mosher, R. Raj, Acta Metall. 22 (1974) 1469–1474.
[13] R.J. O'Connell, B. Budiansky, J. Geophys. Res. 82 (1977) 5719–5735.
[14] T.T. Gribb, R.F. Cooper, J. Geophys. Res. 103 (1998) 27267–27279.
[15] G.M. Mavko, J. Geophys. Res. 85 (1980) 5173–5189.
[16] R.E. Dunin-Borkowski, Ultramicroscopy 83 (2000) 193–216.
[17] A. Lakki, R. Schaller, J. Phys. IV 6 (1996) 331–340.
[18] A. Lakki, R. Schaller, C. Carry, W. Benoit, J. Am. Ceram. Soc. 82 (1999) 2181–2187.
[19] D.R. Clarke, J. Am. Ceram. Soc. 70 (1987) 15–22.
[20] G. Pezzotti, K. Ota, H.-J. Kleebe, J. Am. Ceram. Soc. 79 (1996) 2237–2246.
[21] G. Pezzotti, H.-J. Kleebe, K. Ota, K. Yabuta, J. Am. Ceram. Soc. 80 (1997) 2349–2354.
[22] G. Pezzotti, H.J. Kleebe, K. Ota, J. Am. Ceram. Soc. 81 (1998) 3293–3299.